Validity of the orbital-motion-limited regime of cylindrical probes

J. R. Sanmartín, ETSI Aeronáuticos, Universidad Politécnica de Madrid
28040, Madrid, Spain

R. D. Estes, Harvard-Smithsonian Center of Astrophysics
60 Garden St., Cambridge, MA 02138

Abstract

An asymptotic analysis of electron collection at high bias Φ_p serves to determine the domain of validity of the OML regime of cylindrical Langmuir probes, which is basic for the workings of conductive bare tethers. The breakdown of the regime is found to occur far from the probe, at energies comparable to the ion temperature T_i. The radius of a wire collecting OML current in an unmagnetized plasma at rest cannot exceed a value, R_{max}, that increases with T_i, and exhibits a minimum as a function of Φ_p; at Φ_p values of interest R_{max} is already increasing and is larger than the Debye length λ_{De}. It is also found that 1) the maximum width of a thin tape is $4R_{max}$; 2) the electron thermal gyroradius must be large compared with both R and λ_{De} for magnetic effects to be negligible; and 3) an ion ram energy large compared with kT_i but small compared with $e\Phi_p$ would have a complex but weak effect on R_{max}.

1. Introduction

Each point of an electrodynamic bare tether collects current as if it were part of a cylinder uniformly polarized at the local tether bias *(9)*. This is because of the enormous disparity between tether thickness and collecting length, which lie in the millimeter and kilometer ranges respectively. Bare tether applications rest on the assumption that electron collection occurs in the (optimal) orbital-motion-limited regime of cylindrical probes. It is thus important to determine the parametric domain of orbital-motion-limited (OML) validity.

Since OML current is proportional to the perimeter of the cross section, a large tether current may require a large perimeter. If the crosswise dimension is too large, however, the current will not reach the OML value because of electrical screening effects related to a short plasma Debye length λ_{De}. Here we determine the maximum radius of a cylinder collecting OML current in an unmagnetized plasma at rest, and how it depends on the ion temperatue T_i and the bias Φ_p. Values of the ratio $e\Phi_p/kT_e$ of interest for tethers ($T_e \sim 0.15$ eV, $\Phi_p \sim 400$V) are 10^2 times larger than values previously explored numerically. We also consider the maximum width of a thin tape.

Again, if the crosswise dimension is too large, the current will not reach the OML value because of magnetic guiding effects due to a short thermal electron gyroradius l_e. We consider how large has l_e to be for magnetic effects to be negligible. Finally, we also

study the effects of an ion ram energy large compared with thermal energies but small compared with $e\Phi_p$.

2. Circular cylinder at rest in an unmagnetized plasma

The electron current I to a sufficiently long cylinder in a Maxwellian plasma of density N_∞ and temperatures T_e and T_i, may be written in dimensionless form as

$$\frac{I}{I_{th}} = \text{function of } \frac{R}{\lambda_{De}}, \frac{e\Phi_p}{kT_e}, \frac{T_i}{T_e}. \tag{1}$$

Here, I_{th} is the thermal or random current

$$I_{th} = 2\pi RL \times \frac{1}{4}\sqrt{\frac{8kT_e}{\pi m_e}} eN_\infty \tag{2}$$

where R and L are probe radius and length, and λ_{De} is $\sqrt{kT_e/4\pi e^2 N_\infty}$. In general, the determination of electron trajectories to obtain the current requires solving Poisson's equation for the potential $\Phi(r)$,

$$\frac{\lambda_{Di}^2}{r}\frac{d}{dr}r\frac{d}{dr}\left(\frac{e\Phi}{kT_i}\right) = \frac{N_e}{N_\infty} - \frac{N_i}{N_\infty}, \qquad (\lambda_{Di} = \lambda_{De}\sqrt{T_i/T_e}) \tag{3}$$

with boundary conditions

$$\Phi = \Phi_p > 0 \quad \text{at} \quad r = R, \qquad \Phi \to 0 \quad \text{as} \quad r \to \infty. \tag{4}$$

Both the electric field $-\nabla\Phi$ and the probe acting as a sink of particles affect the densities N_e and N_i, and thus $\Phi(r)$ itself. The basic problem in probe theory usually lies in the attracted-particle density N_e. Actually, for the very large $e\Phi_p/kT_e$ values of interest, the repelled-particle density N_i is accurately given by the simple Boltzmann law,

$$N_i \approx N_\infty \exp(-e\Phi/kT_i), \tag{5}$$

except near the probe where, anyway, N_i is exponentially small (as the ion current itself). Because of Eq.(5), it proves convenient to normalize potential and radius with the ion parameters, T_i and λ_{Di}, although final results may be given in terms of T_e and λ_{De}.

For the highly symmetrical case of this section, the axial velocity v_z (Fig.1) and the transverse angular momentum and energy,

$$J \equiv m_e r v_\theta \ ,$$

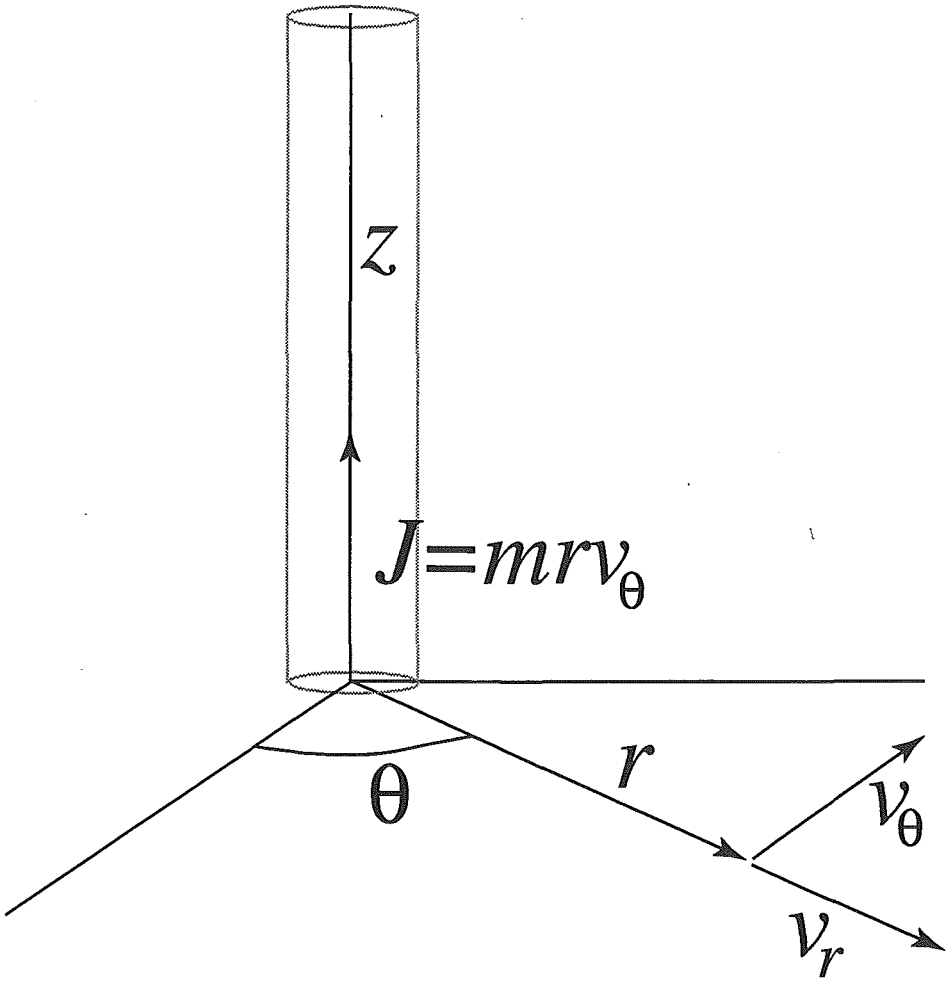

FIGURE 1

$$E \equiv \frac{m_e}{2} v_r^2 + \frac{J^2}{2m_e r^2} - e\Phi(r) , \qquad \left(v_r < 0,\ v_r > 0\right) \tag{6}$$

are conserved along electron orbits. The density N_e at each radius r may then be expressed as an integral of the undisturbed Maxwellian distribution function over appropriate ranges of those 3 constants of the motion *(1)*. After a trivial v_z integration one has

$$N_e = N_\infty \frac{m_e}{2\pi k T_e} \iint \frac{\exp\left(-E / kT_e\right) dE dJ}{m_e \sqrt{J_r^2(E) - J^2}} \tag{7}$$

where we defined

$$J_r^2(E) \equiv 2m_e r^2 [E + e\Phi(r)] . \tag{8}$$

The E-integral, which only covers positive values (all electrons start at infinity), must be carried out once for $v_r < 0$ (incoming electrons) and again for $v_r > 0$ (electrons that have turned outwards at a radius between r and R); the J-integral can be made to cover just positive values by writing $dJ \rightarrow 2dJ$. The E-J domain of integration in Eq.(7) is r-dependent because of both the electric field and the sink effect of the probe:

i) For an incoming electron of energy $E > 0$ to actually reach r, $v_{r'}^2$ must have been positive throughout the entire range $r < r' < \infty$. Using (8) in Eq.(6) for E,

$$m_e^2 r'^2 v_{r'}^2 = J_{r'}^2(E) - J^2,$$

the J-range of integration at that energy will clearly be

$$0 < J < J_r^*(E) \equiv \textit{minimum}\ \{\ J_{r'}(E)\ ;\ r < r' < \infty\ \} ; \tag{9}$$

in general, the minimum occurs at a different r' for a different energy E. If $J_r^*(E)$ differs from $J_r(E)$, those electrons in the range $J_r^*(E) < J < J_r(E)$, for which v_r^2 would be positive, never actually reach r and are thus excluded from the integral in (7) ; we say that there is an effective potential barrier for r, at energy E.

ii) For an E-electron outgoing at r the J-range of integration will be

$$J_R^*(E) < J < J_r^*(E),$$

electrons with $J < J_R^*(E)$ having disappeared in the probe.

Equation (7) may now be written as

$$N_e = N_\infty \int_0^\infty \frac{dE}{kT_e} \frac{\exp\left(-E / kT_e\right)}{\pi} \left[2\sin^{-1} \frac{J_r^*(E)}{J_r(E)} - \sin^{-1} \frac{J_R^*(E)}{J_r(E)} \right], \tag{10}$$

half the first term in the bracket being the $v_r < 0$ contribution. The current itself can be easily found to be

$$I = 2LN_\infty \frac{e}{m_e} \int_0^\infty \frac{dE}{kT_e} \exp(-\frac{E}{kT_e})\, J_R^*(E)\,. \tag{11}$$

We note at this point that, through its dependence on $J_r^*(E)$ [and $J_R^*(E)$], the density N_e is a functional of $\Phi(r)$ and thus cannot be known [for use in solving Eq.(3) for $\Phi(r)$] before the potential itself is found ; this results in a complex, iterative numerical solution of Poisson's equation *(3)*. A hypothetical potential with no barriers at all [$J_r^*(E) = J_r(E)$ for $R \le r < \infty$, $0 \le E < \infty$] would simplify N_e in (10) to a function of both r and the local value $\Phi(r)$,

$$N_e = N_\infty \left[1 - \int_0^\infty \frac{dE}{kT_e} \frac{\exp(-E/kT_e)}{\pi} sin^{-1} \sqrt{\frac{R^2\left(E + e\Phi_p\right)}{r^2\left(E + e\Phi(r)\right)}} \right], \tag{12}$$

and would allow a ready solution of Eq.(3), but has no real interest.

The case of interest here is that corresponding to the maximum possible current in Eq.(11). Since we have $J_R^*(E) \le J_R(E)$, from the definition of $J_r^*(E)$ in (9), current is maximum under condition $J_R^*(E) = J_R(E)$, for $0 < E < \infty$ (no potential barrier for <u>just</u> radius R). This is the orbital-motion-limited (OML) current,

$$I_{OML} = 2LN_\infty \frac{e}{m_e} \int_0^\infty \frac{dE}{kT_e} \exp\left(-\frac{E}{kT_e}\right) \sqrt{2m_e R^2\left(E + e\Phi_p\right)}$$

$$\rightarrow 2RLN_\infty e\sqrt{2e\Phi_p/m_e}\,, \qquad \text{for} \quad e\Phi_p >> kT_e\,. \tag{13}$$

With the current known, there would now be no need for solving Eq.(3), except for the very purpose of the present work: determining the parametric domain for the OML regime to hold. For $e\Phi_p >> kT_e$, this problem comes out to be reasonably simple.

The OML condition, $J_R^*(E) = J_R(E)$ for $0 < E < \infty$, which does reduce the <u>second</u> term in the bracket of (10) to a function of both r and the local value $\Phi(r)$, is readily shown to be equivalent to condition

$$r^2\Phi(r) \ge R^2\Phi_p \qquad (R < r < \infty) \tag{14}$$

on the potential. Condition (14) can be conveniently illustrated by displaying $\Psi \equiv e\Phi/kT_i$ versus $\Psi_p R^2/r^2$ for potential profiles (Fig.2) ; (14) shows that the profile for $R = R_{max}$

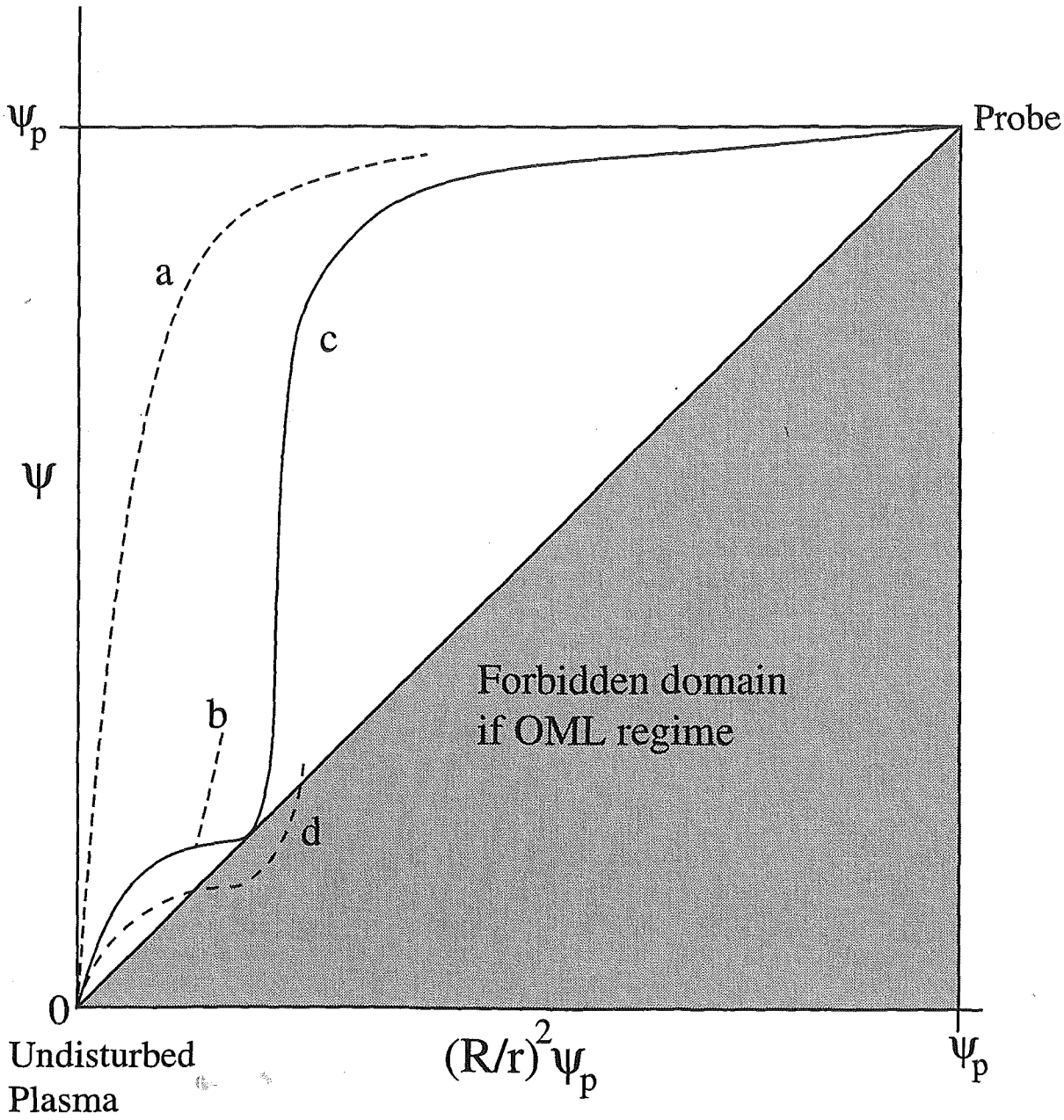
ψ_p
Probe
a
c
ψ
b
d
Forbidden domain
if OML regime
0
Undisturbed
Plasma
$(R/r)^2\psi_p$
ψ_p

FIGURE 2

(maximum radius for the OML regime to hold, with other parameters fixed) would just touch the diagonal in the figure, as in the case of profile *c*. Profiles *a* and *b* would lie in the OML regime, whereas *d* would not.

Next, note that the extreme condition $J_r^*(E) = J_r(E)$ for $R \le r < \infty$, $0 < E < \infty$, which led to Eq.(12), would require the potential to satisfy the condition

$$d(r^2\Phi)/dr \ge 0\,, \qquad (R < r < \infty) \tag{15}$$

which is, of course, more restrictive than (14). In Fig.2 only the hypothetical profile *a* satisfies (15). Note, however, that if $d(r^2\Phi)/dr$ is positive just beyond some radius r_0, then we do have

$$J_r^*(E) = J_r(E) \qquad \text{for } r_0 < r < \infty\,, \quad 0 < E < \infty \tag{16}$$

and Eq.(10) reduces to (12) for $r \ge r_0$; cases *b-d* present this property (0 is the profile point where the tangent goes through the origin).

Figure 3 shows again the qualitative profile *c* of Fig.2, which we find corresponds to the actual profile for $R = R_{max}$ at large $\Psi_p \equiv e\Phi_p/kT_i$; this may be taken as an ansatz that is used in solving Poisson's equation and verified at the end. Below, we sketch our asymptotic analysis of Eq.(3) for $\Psi_p >> 1$, following closely a classical study *(5)*, which assumed, however, a monoenergetic attracted-particle distribution function, and was developed for the non-OML, small λ_{Di}/R, regime :

i) Both the quasineutral approximation, $N_e \approx N_i$, and the no barrier condition, $J_r^*(E) = J_r(E)$, hold below point 0. Use of Eqs.(5) and (12) determines point 0 exactly.

ii) The quasineutral approximation remains valid up to a point 1 where $d\Phi/dr \to \infty$. This property of point 1, and the proximity of values r_0 and r_1, make possible to get an accurate approximation to the potential barrier (and the density N_e) for points in the vicinity of 1, which can then be determined. The same barrier applies to points above 1, i.e., for $r < r_1$ we have $J_r^*(E) = J_{r_1}^*(E) \equiv$ *minimum* $[J_{r'}(E), r_1 < r' < r_0, 0 < E < \infty]$.

iii) Above point 1 there are two thin, non-quasineutral layers that take the solution to a radius r_2 a bit closer to the probe, and to values Φ satisfying $\Phi_1 << \Phi << \Phi_p$.

iv) Finally, a solution to Poisson's equation (with N_i negligible) that matches the inner thin layer at r_2 and satisfies condition $\Phi = \Phi_p$ at $r = R$, yields a relation between parameters, i.e. determines R_{max}.

Note that both Ψ_0 and Ψ_1 are of order unity whereas Ψ_p is very large ($\sim 10^3, 10^4$). Hence, if Fig. 3 were drawn on scale, the near-vertical potential drop in the two thin layers, down to point 1, would occur very close to the Ψ-axis, and point 0 would lie very close to the origin. With $e\Phi_0$, $e\Phi_1 \sim kT_i$, the ion temperature should critically affect OML validity.

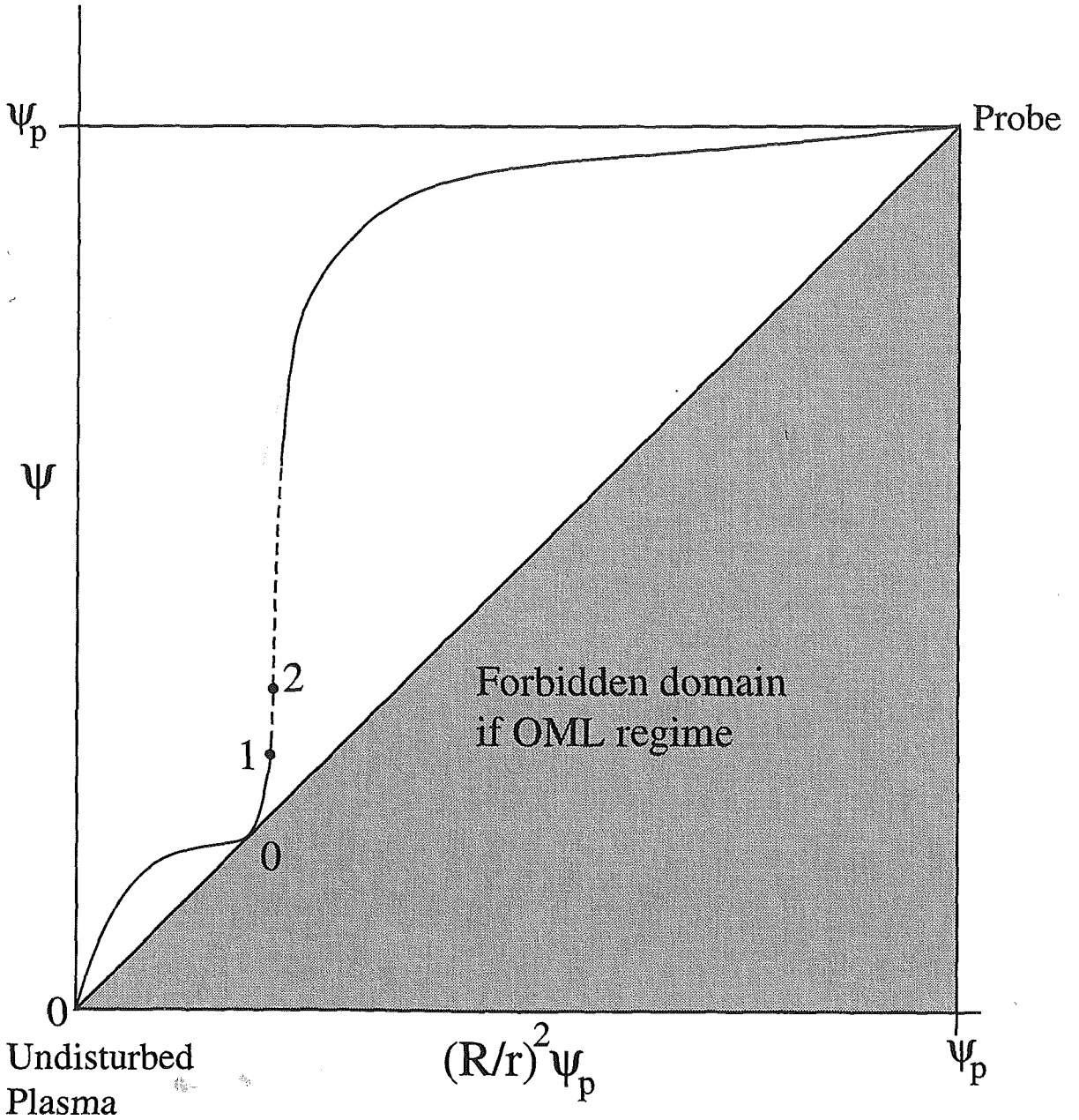
ψ_p
Probe
ψ
2
1
0
Forbidden domain
if OML regime
0
Undisturbed
Plasma
$(R/r)^2\psi_p$
ψ_p

FIGURE 3

Note also that the high probe bias ($\Psi_p >>1$) makes space-charge effects negligible within some neighborhood of the probe (even if R is not small compared with Debye lengths). Within that neighborhood, and ignoring N_e - N_i in Eq.(3), $\Phi(r)$ behaves as a (logarithmic) solution to the 2D Laplace-equation,

$$\Phi = \Phi_p[1-\alpha \ln (r/R)] , \tag{17}$$

α being a moderately small constant (of order $1/\ln\Psi_p$).

Figure 4 shows R_{max}/λ_{De} versus $e\Phi_p/kT_e$ for the ionospheric case, $T_i/T_e \approx 1$; R_{max} goes through a minimum as the bias Φ_p increases and, at high enough Φ_p, exceeds λ_{De}. Numerical results for the range $e\Phi_p / kT_i < 25$ had shown R_{max} decreasing monotonically with the bias *(3)*. Figure 5 shows that R_{max} does increase sensibly with T_i.

3. **Thin tape at rest in an unmagnetized plasma**

In the OML regime, the current to a cylindrical probe is independent of the shape of the cross section; it just depends on its perimeter *(4)*. The limits of OML validity, however, must be determined anew for every cross section. Since angular momentum J is not conserved here, there is no close-form expression such as (10) for N_e. Nonetheless, we find that the high bias condition ($\Psi_p >>1$) makes possible to approximately reduce this problem to the case of the circular cylinder.

We use here elliptical coordinates v and w (see Fig.6, where we set $a = 1$),

$$x = a \cos v \cosh w , \qquad y = a \sin v \sinh w,$$
$$(0 \le v < 2\pi , \quad 0 \le w < \infty) ,$$

Poisson's equation then reading

$$\frac{\lambda_{Di}^2}{a^2(\sinh^2 w + \sin^2 v)}\left(\frac{\partial^2\Psi}{\partial w^2}+\frac{\partial^2\Psi}{\partial v^2}\right) = \frac{N_e}{N_\infty} - \exp(-\Psi). \tag{18}$$

The ellipses $w(x,y)$ = *constant* approach circles as w increases; at large radial distances one has

$$w = \ln\frac{r}{a} + \ln 2 - \frac{x^2 - y^2}{4r^2}\frac{a^2}{r^2} + \ldots \tag{19}$$

We may reasonably use the approximation $w = \ln(2r/a)$ for $w > w^*$, with $w^* = 1.25$ or 1.5, say. Note also that the limit ellipse $w = 0$ is the segment $y = 0$, $-a < x < a$, which may represent the cross section of a tape of width $2a$ and negligible thickness.

FIGURE 4

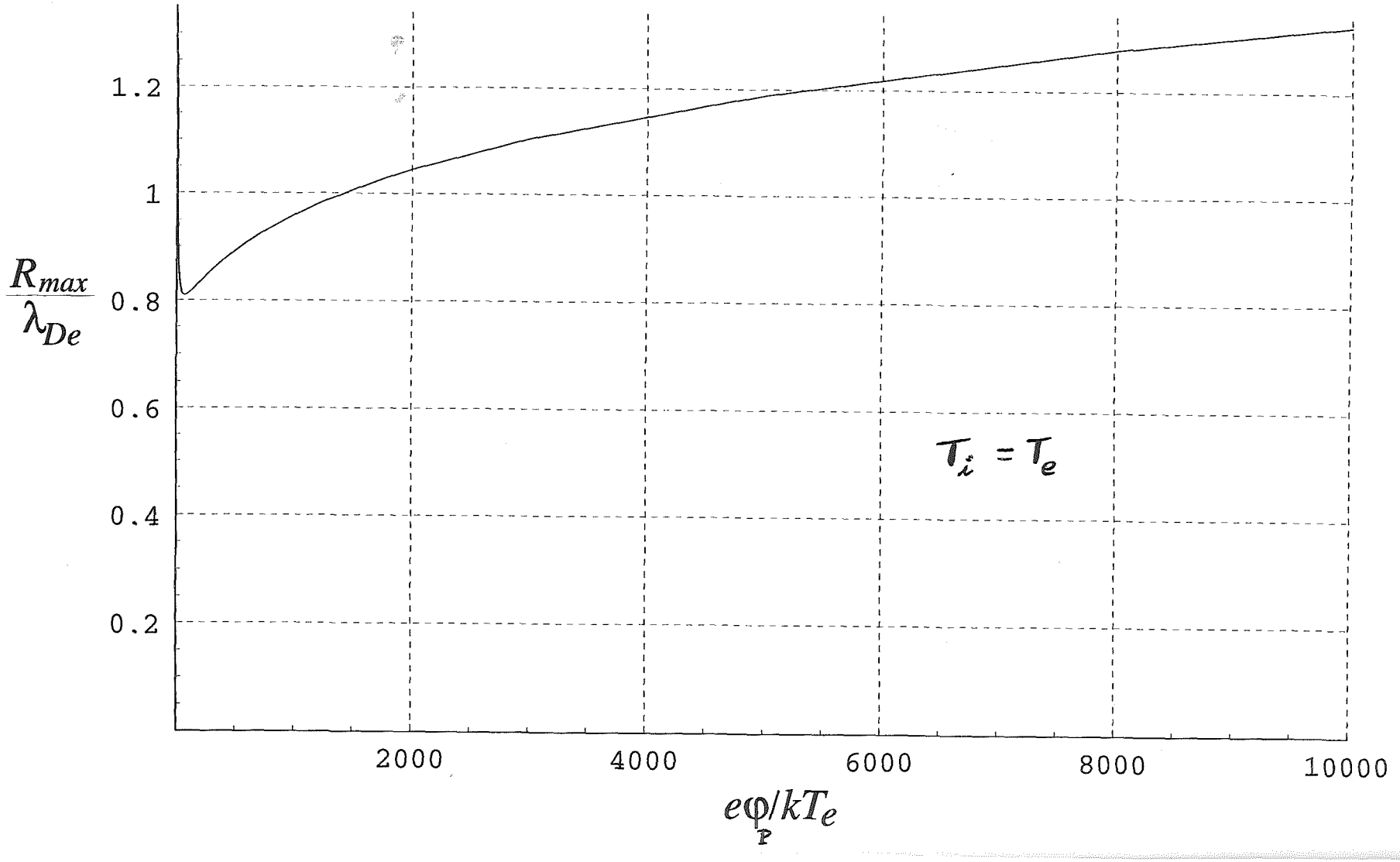
1.2
1
0.8
0.6
0.4
0.2
$\frac{R_{max}}{\lambda_{De}}$
2000
4000
6000
8000
10000
$e\varphi_p/kT_e$
$T_i = T_e$

FIGURE 5

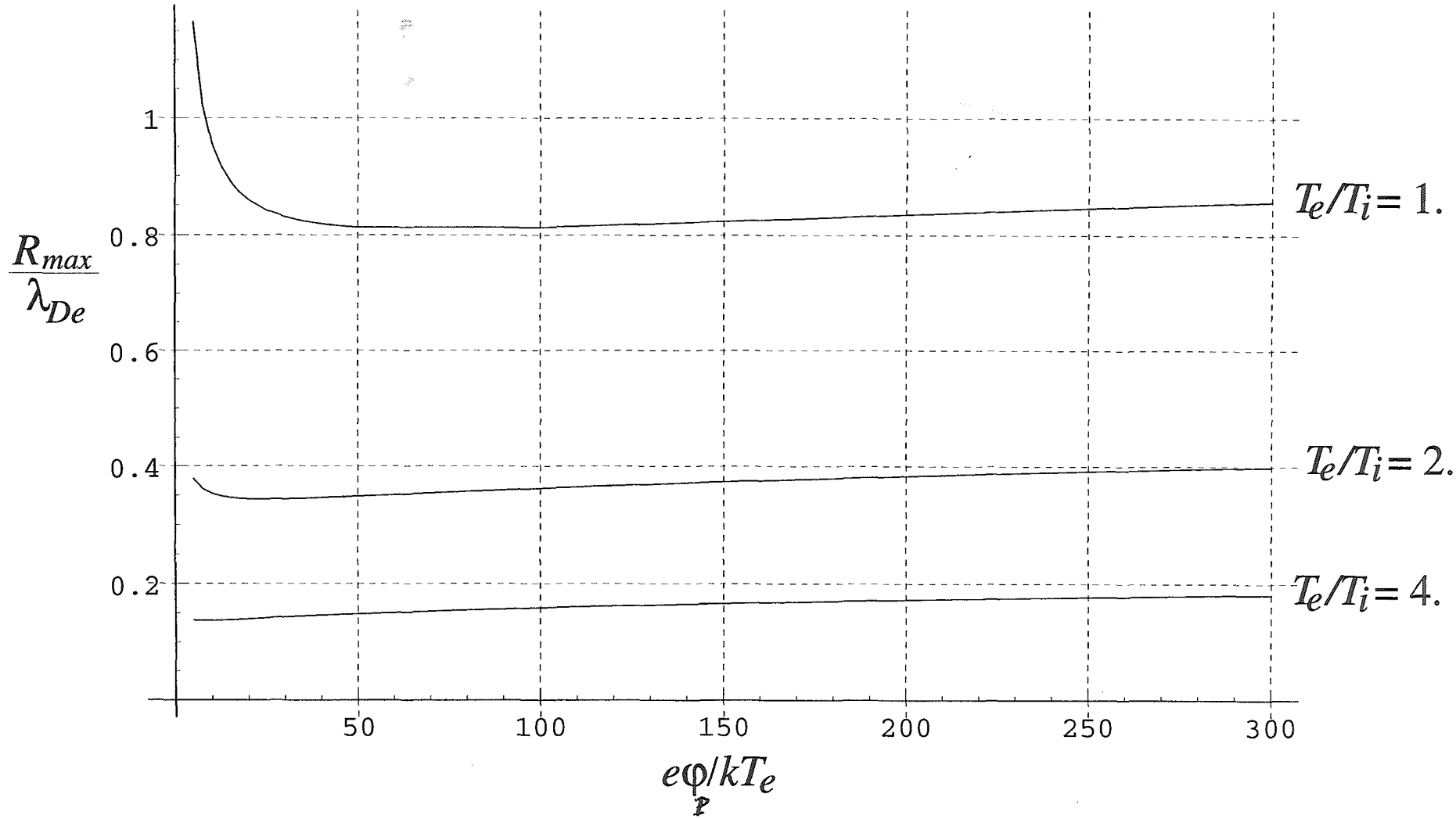
$\frac{R_{max}}{\lambda_{De}}$
1
0.8
0.6
0.4
0.2
50
100
150
200
250
300
$e\varphi_p/kT_e$
$T_e/T_i = 1.$
$T_e/T_i = 2.$
$T_e/T_i = 4.$

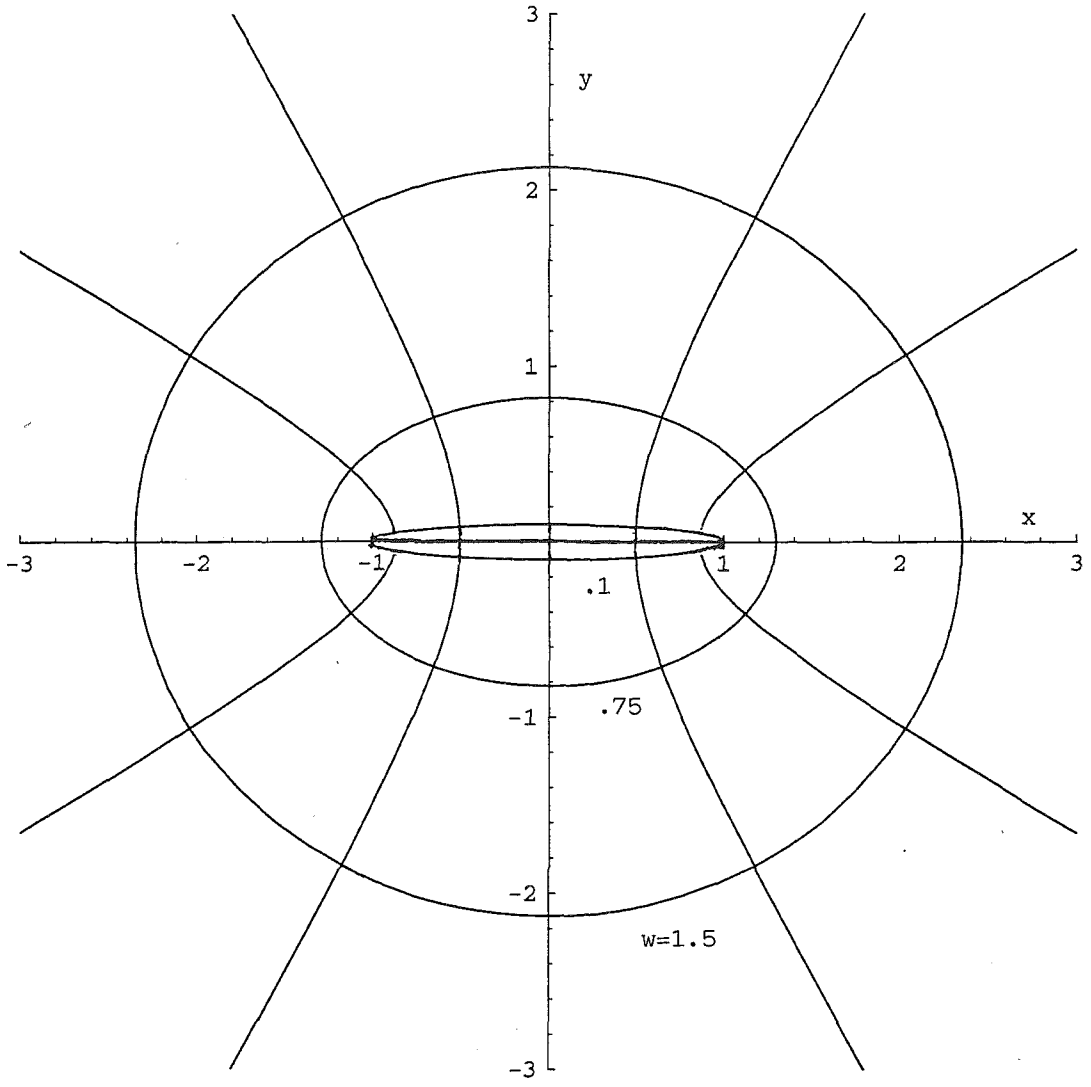

FIGURE 6

As in the previous section, the space-charge may be ignored in some neighborhood of the probe, which, for Ψ_p large enough, extends into the region where w-ellipses are near-circles, that is, beyond $w = w^*$. We may then argue that the potential Ψ will be nearly independent of v everywhere, i.e. $\Psi(w, v) \approx \Psi(w)$ (and the electric field at $w > w^*$ will be radial) in the following way :

i) The electron density for $w > w^*$ would then be a function of just w, $N_e = N_e(w)$. This is because, at a point in that region, incoming electrons, and outgoing electrons that did not reach values $w < w^*$, find a radial field throughout their motion and conserve the angular momentum J ; their contribution to N_e will be a function of r, and thus, of w. Those outgoing electrons that had reached values $w < w^*$ and missed the probe, have J changed by a quantity ΔJ that is small ($\Delta J \sim J/\ln\Psi_p$) as a result of the shallow (logarithmic) character of the potential in the vicinity of the probe, where the field is not radial; their contribution to N_e will be weakly dependent on v. On the whole we would have $N_e \approx N_e(w)$.

ii) Poisson's equation reads

$$\frac{\partial^2\Psi}{\partial^2 w} + \frac{\partial^2\Psi}{\partial^2 v} \approx 0 \tag{20a}$$

for $w < w^*$, and

$$\frac{\lambda_{Di}^{\,2}}{a^2 \sinh^2 w}\left(\frac{\partial^2\Psi}{\partial^2 w} + \frac{\partial^2\Psi}{\partial^2 v}\right) \approx \frac{N_e}{N_\infty} - \exp(-\Psi) \tag{20b}$$

for $w > w^*$, with some overlapping range of validity. In neither (20a) nor (20b) does v show up explicitly.

iii) Finally, boundary conditions refer to just w,

$$\Psi = \Psi_p \quad \text{at} \quad w = 0, \qquad \Psi \to 0 \quad \text{as} \quad w \to \infty.$$

With $\Psi = \Psi(w)$, and $w = \ln(2r/a)$ for $w > w^*$, we now have :

1) Equation (20a) and the probe boundary condition yield

$$\Psi = \Psi_p[1 - \beta\, w] \tag{21}$$

$$\to \Psi = \Psi_p\left[1 - \beta \ln\left(\frac{r}{a/2}\right)\right] \quad \text{for } w > w^*. \tag{22}$$

2) Equation (20b) for $w > w^*$ recovers (3), whose solution, as in Fig.3 of section 2, will show an outer quasineutral region, thin layers, and a broad, ion-free, inner region. This solution, rather than satisfying the boundary condition at the probe, must match smoothly the behavior given in (22), within the overlapping range of validity. Comparing

Eqs.(17) and (22) shows that, beyond w^*, the solution behaves as in the case of a circular cylinder with an effective radius $R = a/2$ (the coefficients β and α being equal).

This suggests that, with all other parameters given, the maximum width of a thin tape in the OML regime relates quite simply to the maximum radius of a circular cylinder,

$$2a_{max} = 4R_{max}. \tag{23}$$

Note that, since OML current is proportional to the perimeter, use of a tape would only increase the maximum current by a factor $4/\pi$, or 27 %. A tape might be actually preferable for other reasons: a cylinder with R_{max} might be too heavy and rigid *(7)*; a tape may lead to a shorter tether *(2)*. The main interest of the result is then that the maximum half-width of a tape is twice R_{max} as given in Figs. 4 and 5.

One must still take into account the fact that the Laplace potential (21), for the region $w < w^*$, is quite different from the potential (17). It then comes out that a tape, contrary to a circular cylinder, never collects the full OML current, although this has no practical consequences. There are potential barriers in the vicinity of any flat collecting surface, the effects being weak, however, in the case of a shallow 2D Laplace potential *(4)*. Using (21) we find that potential barriers around the tape lie in a thin region of thickness $\sim a/\ln\Psi_p$, and that current reduction below the OML value is of order $(1/\ln\Psi_p)^2$, or about 1 %. Equation (23) should then properly read that current to a tape keeps very close to the OML value for $a \leq 2R_{max}$.

4. Circular cylinder at rest in a magnetized plasma

As in the previous section, there is no closed-form expression for N_e in the presence of an uniform magnetic field $\boldsymbol{B}$, which allows for only two constants of the motion, energy and canonical angular momentum. Overall use of these two constants leads to the Parker-Murphy current law, which takes the character of an upper bound at the high bias of interest *(6)*. For $e\Phi_p >> kT_e$ and cylindrical geometry one has

$$I_{PM} \approx I_{OML}\sqrt{\pi/2} \times l_e/R\,, \tag{24}$$

where l_e is the electron thermal gyroradius

$$l_e \equiv v_{th}/\Omega_e \propto 1/B \qquad (v_{th} \equiv \sqrt{kT_e/m_e}, \quad \Omega_e \equiv eB/m_e).$$

Equation (24) suggests that if R/l_e is small, I_{OML} then lying well below the I_{PM} bound, the OML current will hardly be affected by magnetic effects.

To get more definite results, we consider the exact equations for electron motion in the presence of the electric field due to probe and plasma, $-\nabla\Phi(x, y)$ [probe and z axes

coincide], and an uniform magnetic field B perpendicular to the probe, say along the y-axis:

$$\frac{d^2 v_x}{dt^2} + \Omega_e^2 \left[1 - l_e^2 \frac{\partial^2}{\partial x^2} \left(\frac{e\Phi}{kT_e} \right) \right] v_x = v_{th}^2 v_y \frac{\partial^2}{\partial x \partial y} \left(\frac{e\Phi}{kT_e} \right) , \tag{25a}$$

$$\frac{dv_y}{dt} = v_{th}^2 \frac{\partial}{\partial y} \left(\frac{e\Phi}{kT_e} \right), \tag{25b}$$

$$\frac{d^2 v_z}{dt^2} + \Omega_e^2 v_z = -v_{th}^2 \Omega_e \frac{\partial}{\partial x} \left(\frac{e\Phi}{kT_e} \right). \tag{25c}$$

Equations (25a and c) were obtained by deriving the respective equations of motion and using the derivative along the electron orbit *(10)*,

$$\frac{dE_x}{dt} = \frac{\partial E_x}{\partial x} v_x + \frac{\partial E_x}{\partial y} v_y ,$$

The last two terms of (25c) would give the usual E/B drift; the first two terms represent gyromotion. The important equation is (25a), which should describe the approach to the probe across field lines.

The left-hand side of (25a) would again represent gyromotion if the second term in the bracket were small, that is for B large enough (l_e small enough). Assuming, on the contrary, that l_e is sufficiently large, we neglect the first (gyromotion) term and use the $B = 0$ solution of section 2 to determine how small must be the magnetic field for the second term in the bracket to be indeed large. In the broad region between probe and thin layers of Fig.3, the resulting condition is, basically, that the R/l_e ratio of the Parker-Murphy law (24) be small ; in particular, near the probe, where both Eq.(17) and the approximation

$$\frac{d^2 \Phi}{dr^2} \approx -\frac{1}{r} \frac{d\Phi}{dr}$$

hold, the left-hand-side of Eq.(25a) takes the simple form

$$\frac{d^2 v_x}{dt^2} + \Omega_e^2 \left[1 - \frac{l_e^2}{R^2} \left(\frac{R^2}{r^2} \frac{x^2 - y^2}{r^2} \alpha \frac{e\Phi_p}{kT_e} \right) \right] v_x$$

with the first 3 factors in the parenthesis moderately small, and the last factor large. In the quasineutral region of Fig.3, the second term in the bracket is never large for $T_i \approx T_e$, but

the electrons are then hardly affected by the potential before they reach r_0 ($e\Phi_0 \approx 0.194\ kT_e$). Finally, in the two thin layers, where we have $N_e - N_i \sim N_\infty$ and

$$\frac{d^2\Phi}{dr^2} << \frac{-1}{r}\frac{d\Phi}{dr},$$

the left-hand-side becomes

$$\frac{d^2 v_x}{dt^2} + \Omega_e^2 \left[1 - \frac{l_e^2}{\lambda_{De}^2}\frac{x^2}{r^2}\frac{N_e - N_i}{N_\infty} \right] v_x$$

This means that for B-effects to be negligible, both R/l_e and λ_{De}^2/l_e^2 must be small.

At the relatively high densities of the F-layer, $\lambda_{De}^2/l_e^2 \propto B^2/N_\infty$ is indeed small (about 10^{-2} and 10^{-1} for $N_\infty = 10^{12}$ and 10^{11} m^{-3}, respectively), but it reaches above unity at extreme altitudes. Experiments on board an elliptical-orbit satellite *(8)* and a rocket *(11)* did show a current dependent on the angle between $\boldsymbol{B}$ and a cylindrical probe (B-effects) when N_∞ dropped low enough, at very low and high altitudes. In all cases probe bias was only moderately high.

5. Circular cylinder moving through an unmagnetized plasma

The case of interest is that of a large ion ram energy,

$$\tfrac{1}{2}\, m_i U^2 >> kT_i,$$

where U is the plasma velocity past the probe ; for a tether orbiting in the F layer (oxygen ions, orbiting velocity) we have indeed $\tfrac{1}{2}\, m_i U^2 \approx 4.5$ eV $>> kT_i \sim 0.15$ eV. The unperturbed ion distribution function is now non isotropic and the electric field non radial, but the OML current law, which is independent of both ion distribution and cross section shape, is still valid. The high-bias limit law (13) is particularly robust : it is also independent of the unperturbed electron distribution function as long as it is isotropic, which is the case here ($\tfrac{1}{2}\, m_e U^2 << kT_e$).

The ion ram energy could affect, however, the domain of validity of the OML law. For the case of interest, $\tfrac{1}{2}\, m_i U^2 << e\Phi_p$, ions would be kept far away from the probe for all directions, with an (angle dependent) potential structure similar to that shown in Fig.3. For all other parameters fixed, the distance r_1 (or r_2) in Fig.3 is directly related to the characteristic ion energy. In a plasma with $T_i = T_e$, a crude model suggests the distances would correspond to an effective ion temperature $kT_i(eff) = \tfrac{1}{2}\, m_i U^2$ on the windward side, and $T_i(eff) = T_e$ on the lateral sides; when particularised for a small ratio T_i/T_e, the analysis sketched in section 2 would roughly give $T_i(eff) \sim T_e \times \sqrt{kT_e/(\tfrac{1}{2}\, m_i U^2)}$ for the lee side. Since R_{max} increases with T_i/T_e (Fig.5), a wire with $R = R_{max}(U = 0,$

$T_i/T_e = 1$) would collect current in agreement with the OML law at the lateral sides and at the front, and below the OML level at the lee side; a preliminary analysis of how the current lags behind the OML value as R increases beyond R_{max} shows, however, that I/I_{OML} keeps closer to 1 the lower the ratio T_i/T_e. A wire with $R = R_{max}(U = 0, T_i/T_e = 1)$ should then collect current very close to the law (13).

We note finally that conditions in laboratory plasmas may substantially differ from those applying in the tether case. The ratio T_i/T_e is usually small and, as a consequence of Fig.5, cylindrical probes will collect current below the OML value unless R is well below λ_{De}. Also, in flowing laboratory plasmas the ion ram energy may be comparable to the bias applied at the probe, $\frac{1}{2} m_i U^2 \sim e\Phi_p$; again, unless R is much less than λ_{De}, the potential would be non monotonic, with an overshoot at the front and a trough on the lee side, and the prediction of current would be difficult.

6. Conclusions

Bare tether applications are based on the assumption that the tether collects electrons in the OML regime of cylindrical Langmuir probes. The definite and simple OML current law, which allows for detailed design considerations, has opened the way to a technology of electrodynamic tethers *(2)*. Here, we have determined the domain of OML validity in parameter space; we studied the surface bounding that domain as a relation among the dimensionless numbers

$$R/\lambda_{De},\quad e\Phi_p/kT_e,\quad T_i/T_e,\quad \tfrac{1}{2}m_iU^2/kT_i,\quad \text{and}\quad \lambda_{De}/l_e\,,$$

for the very large $e\Phi_p/kT_e$ values of interest. (The mass ratio m_e/m_i enters through the irrelevant numbers $\frac{1}{2}m_eU^2/kT_e$ and λ_{De}/l_i.)

We found that the ratio λ_{De}/l_e (actually, λ_{De}^2/l_e^2) must be small for magnetic effects -which would break the OML law otherwise- to be ignorable. This ratio is a property of the plasma rather than a free design parameter. In the Earth's ionosphere λ_{De}^2/l_e^2 is small for N_∞ clearly above 10^{10} m^{-3}; this breaks down at low, and sufficiently high, altitudes.

For λ_{De}^2/l_e^2 small, and first taking $\frac{1}{2}m_iU^2/kT_i \sim 0$, we determined the maximum radius for the OML regime to hold, giving

$$R_{max}/\lambda_{De} \quad versus \quad e\Phi_p/kT_e,\ \text{and}\ T_i/T_e\,.$$

R_{max} exibits a minimum as a function of Φ_p but, at the bias of interest, is slowly increasing, and above λ_{De} in the ionospheric case ($T_i/T_e \sim 1$). For λ_{De}^2/l_e^2 small and $R \sim \lambda_{De}$, we have R^2/l_e^2 small too, a second condition we found required for magnetic effects to be weak. We also found R_{max}/λ_{De} increasing with T_i/T_e.

We finally found that if

$$\tfrac{1}{2}m_iU^2/kT_i \times T_i/T_e \times kT_e/e\Phi_p = \tfrac{1}{2}m_iU^2/e\Phi_p$$

is small, as in the tether case, the ion ram energy $\tfrac{1}{2}m_iU^2$ will only affect the potential structure far away from the probe. This structure reaches a distance that depends on the ion characteristic energy, the ram energy making that distance angle-dependent. Both the increase of R_{max} with T_i/T_e (for vanishing U), and the fact that, at low T_i/T_e, the current hardly lags behind the OML value as R exceeds R_{max}, indicate that a wire with $R \leq R_{max}(U = 0, T_i/T_e = 1)$ would collect current very close to the OML value.

If a thin tape is used instead of a wire (with all others parameters equal), the maximum valid width is found to be $4R_{max}$.

Acknowledgments

The work of J.R.Sanmartín was supported by DGYCIT (Spain) under grant PB94-0417-C03-01.

References

1. Bernstein, I.B. and Rabinowitz, I.N., Theory of electrostatic probes in a low-density plasma, *Phys. Fluids* 2, 1959, 112-121.

2. Johnson, L., Carroll, J., Estes, R., Gilchrist, B., Lorenzini, E., Martínez-Sanchez, M., Sanmartín, J.R., and Vas, I., Electrodynamic tethers for reboost of the international space station and spacecraft propulsion, paper presented at the *AIAA Space Programs and Technologies Conference*, Am. Inst. of Aeronautics and Astronautics, Huntsville, Ala., Sept. 1996.

3. Laframboise, J.G., Theory of spherical and cylindrical Langmuir probes in a collisionless, Maxwellian plasma at rest, University of Toronto Institute of Aerospace Studies Report No.100, June 1966.

4. Laframboise, J.G. and Parker, L.W., Probe design for orbit-limited current collection, *Phys. Fluids* 16, 1973, 629-636.

5. Lam, S.H., Unified theory for the Langmuir probe in a collisionless plasma, *Phys. Fluids* 8, 1965, 73-87.

6. Parker, L.W. and Murphy, B.L., Potential buildup on an electron-emitting ionospheric satellite, *J. Geophys. Res.* 72, 1967, 1631-1636.

7. Martínez-Sanchez, M. and Sanmartín, J.R., Artificial auroral effects from a bare conducting tether, *J. Geophys. Res.* 102, 1997 (in press).

8. Miller, N.J., Some implications of satellite spin effects in cylindrical probe measurements, *J. Geophys. Res.* 77, 1972, 2851-2861.

9. Sanmartín, J.R., Martínez-Sanchez, M., and Ahedo, E., Bare wire anodes for electrodynamic tethers, *J. Propul. Power* 9, 1973, 353-360.

10. Singh, N. and Chaganti, V.S., Electron collection by a highly positive satellite in the ionosphere: Test particle simulation, *J. Geophys. Res.* 99, 1994, 469-478.

11. Szuszczewicz, E.P. and Takacs, P.Z., Magnetosheath effects on cylindrical Langmuir probes, *Phys. Fluids* 22, 1979, 2424-2429.